remote sensing

MDPI

Article

Leaf Surface Reflectance Does Not Affect Biophysical Traits Modelling from VIS-NIR Spectra in Plants with Sparsely Distributed Trichomes

Eva Neuwirthová [1], Zuzana Lhotáková [1], Petr Lukeš [2] and Jana Albrechtová [1,*]

[1] Department of Experimental Plant Biology, Faculty of Science, Charles University, Viničná 5, 12844 Praha, Czech Republic; eva.neuwirthova@natur.cuni.cz (E.N.); zuzana.lhotakova@natur.cuni.cz (Z.L.)
[2] Global Change Research Centre, Academy of Science of the Czech Republic, Bělidla 4a, 60300 Brno, Czech Republic; lukes.p@czechglobe.cz
* Correspondence: jana.albrechtova@natur.cuni.cz; Tel.: +420-221-951-659

Abstract: In this study, we examine leaf reflectance as the main optical property used in remote sensing of vegetation. The total leaf reflectance consists of two main components: a diffuse component, originating from the leaf interior, and a component reflected directly from the leaf surface. The latter contains specular (mirror-like) reflectance (SR) and surface particle scattering, driven by the surface roughness. Our study aimed to (1) reveal the effects of key leaf structural traits on SR in 400–2500 nm, and (2) compare the performance of PLSR models of leaf biophysical properties based on the total reflectance and SR removal reflectance. Four *Arabidopsis thaliana* structural surface mutants and six *Hieracium* species differing in trichome properties were studied. PCA did not reveal any systematic effect of trichome density, length, and morphology on SR. Therefore, the results do not support the hypothesis that leaves with denser and longer trichomes have lower SR and higher total reflectance than the smooth leaves. SR removal did not remarkably improve PLSR models of biophysical traits (up to 2% of RMSE). Thus, in herbaceous dorsiventral leaves with relatively sparse trichomes of various morphology and without apparent waxy surface, we cannot confirm that SR removal significantly improves biophysical trait prediction.

Keywords: diffuse reflectance; integrating sphere; leaf anatomical traits; leaf epidermal structure; specific leaf area; specular reflectance; trichome parameters; laboratory spectroscopy

check for updates

Citation: Neuwirthová, E.; Lhotáková, Z.; Lukeš, P.; Albrechtová, J. Leaf Surface Reflectance Does Not Affect Biophysical Traits Modelling from VIS-NIR Spectra in Plants with Sparsely Distributed Trichomes. *Remote Sens.* **2021**, *13*, 4144. https://doi.org/10.3390/rs13204144

Academic Editor: Fernando Camacho

Received: 22 September 2021
Accepted: 14 October 2021
Published: 16 October 2021

Publisher's Note: MDPI stays neutral with regard to jurisdictional claims in published maps and institutional affiliations.

Copyright: © 2021 by the authors. Licensee MDPI, Basel, Switzerland. This article is an open access article distributed under the terms and conditions of the Creative Commons Attribution (CC BY) license (https://creativecommons.org/licenses/by/4.0/).

1. Introduction

Leaf optical properties, i.e., reflectance, absorbance, and transmittance, are defined as the fractions of incoming light that are reflected, absorbed, and transmitted by a leaf, respectively. Leaf reflectance as the main optical property used in the evaluation of vegetation status on a large scale using remote sensing approaches [1] and plant phenotyping [2,3].

Glossy green leaves may appear white in some view directions, meaning they have a strong reflectance in one specific direction compared to others [4,5]. This simple observation demonstrates that the leaf reflectance exhibits an angular dependency on incident and viewing angle [6]. A previous assumption that a leaf acts as a Lambertian reflector (meaning that reflected light is perfectly diffused and constant in all directions) has been rejected by many earlier studies, including [7,8].

The light reflected from a leaf consists of two components with different origins. First, the radiation reflected from a leaf interior, which is diffuse and determined primarily by leaf biochemical components, water content [1,9], intercellular air spaces [10,11], and the orientation of cell walls [12] in the leaf mesophyll. Second, the radiation reflected from a leaf surface, which is independent of leaf internal composition and structure, and is determined by the surface properties of the epidermis. Light reflected at an angle equal to the angle of incidence produces specular (mirror-like) reflection [13]. This specular fraction of leaf

reflectance, in particular, contributes to the bias from a Lambertian reflection model [14]. The light scattered on very small particles (comparable in size to the wavelength of incident light) at the leaf surface is reflected away from the specular direction and is likely neglected in most plant studies [15].

Separation of the specular component from the diffuse reflectance can be achieved by various optical methods. In the case of bidirectional reflectance factor measurement [16], it is typical to use optical devices measuring the degree of light polarisation [15,17–19], as the light reflected from the leaf surface is polarised in comparison to the diffuse light reflected from inside of the leaf [5]. Another common measurement set-up for bidirectional spectra measurements is placing a sensor at an angle equal to that of the incident light source [20]. If the light reflected from a leaf is integrated over the whole hemisphere using an integrating sphere, the specular component can be removed by placing a specular exclusion light trap at the designated angle of incidence [21].

Because specular reflectance does not contain information from the leaf interior, it was considered a possible source of error in the retrieval of leaf biochemical compounds [18]. The idea of removing the specular component of reflectance from vegetation indices has been investigated for decades [22–24]. Recently, improved chlorophyll content estimation after removing the specular reflectance from total reflectance was achieved [18]. Efforts have also been made to model the specular component in the PROSPECT leaf-level radiative transfer model [25], or to include leaf surface parameters and their effects in the PROSPECT model [26].

Due to the lack of interactions with light-absorbing pigments, specular reflectance is assumed to be constant in visible (VIS) wavelengths [18] with a tendency to increase through the near-infrared spectral region [27,28]. Specular reflectance strongly depends on the angle of incident light [8,29]. McClendon [20] investigated the specular reflectance of several trees, shrubs, and herbs with different epidermal anatomy in the wavelengths around 632 nm. Regardless of the character of leaf surface (waxy, glabrous, or hairy), the specular reflection was several folds higher than the diffuse reflection. The authors of [15] also studied the effect of leaf surface on specular reflectance and showed that the less hairy and glabrous leaves had noticeably higher specular reflectance in comparison to densely pubescent leaves with lower specular reflectance. The undulation of leaf surface and venation has been shown to increase specular reflectance [15]. The effect of epidermal surface properties on reflectance in VIS and near-infrared (NIR) spectral regions was recently explored using measurements from multiple angular geometries [18,27,30] on leaves with very distinct surface properties: leathery, smooth, and shiny; intermediate epidermal roughness with venation or sparse trichomes; and finally, leaves with rough undulating surface and denser trichomes. The three studies confirmed that the apparently smooth and shiny leaves show their sharp maximal reflection peak in the specular viewing direction, i.e., having equal incident and viewing angles. This peak of reflection in the specular direction was almost absent in rough leaves with trichomes. However, epidermal traits were not quantified in any of the above cited studies, and only qualitative measures of leaf surface were used.

From an ecophysiological point of view, leaf optical properties may reflect an adaptation to a particular environment and contribute to efficient water relations and light capture. Understory species have relatively high photosynthetic rates under diffuse light, and exhibit decrease in the photosynthetic rate when wet [31]. Vanderbilt [32] proposed that the specular reflectance originates from cuticle and waxes, which also have water repulsion functions at the leaf surface [33]. The golden surface shine of *Tradescantia* leaves was proven to exhibit specular reflectivity from epidermal nanostructures having a photoprotection purpose [34]. Greater light scattering caused by trichomes was hypothesised by Gates and Tantraporn [35] and confirmed by Qiu et al. [26] as a protection mechanism against excessive photosynthetically active radiation [36].

To assess the influence of trichomes on leaf optical properties, some authors have measured optical properties on hairy leaves before and after removing trichomes [36–39];

however, this may have resulted in artifacts caused by the removal of trichomes. The results were, nevertheless, ambiguous regarding the trichome effect on the reflectance along the VIS–NIR spectrum range. Gausman and Cardenas [37] observed a reflectance drop in the range of 750–1000 nm, which they explained by both trichome removal and loss of phenolic compounds due to trichome shaving.

The aims of our study were: (1) to investigate the effects of selected quantitative epidermal traits (trichome density and length, and adaxial epidermis thickness) on specular reflectance in visible and near-infrared spectral regions, and (2) to compare the performance of partial least squares regression (PLSR) prediction models of leaf biophysical properties based on the total reflectance and the reflectance after specular component removal. To avoid artefacts caused by trichome removal, the study was conducted on intact leaves of two groups of plants with different surface variability: (1) four selected *Arabidopsis thaliana* surface structural mutants, and (2) six selected *Hieracium* species with various trichome density and morphology. We hypothesised that the epidermal traits affect the specular reflectance and that leaves with denser and longer trichomes have lower specular and higher total reflectance than the smooth leaves with fewer or no trichomes. We expected that the exclusion of leaf specular reflectance would improve the performance of PLSR models for leaf biochemical traits estimation.

2. Materials and Methods

2.1. Plant Material and Anatomical Structure Assessment

Two narrow taxonomical groups of the herbaceous plant genus (*A. thaliana* and *Hieracium* species) with dorsoventral leaf anatomy were selected to minimise the variation in other leaf traits but epidermal surface structure. We used closely related taxonomic units to ensure comparable leaf internal structure and minimise the influence of internal structural and biochemical traits on leaf optical properties.

2.1.1. Plant Material and Cultivation

We studied the anatomical and optical properties of wild type (WT, *Columbia-0*) and four structural mutants (*exo70h4-1*, *tbr1*, *arpc5*, and *gl1*) of *Arabidopsis thaliana* (L.) Heynh. (Table 1).

Table 1. Leaf epidermal structural traits of studied plants: wild type *Columbia-0* and four *A. thaliana* structural mutants, with descriptions of surface structural mutation from a referenced study.

***A. thaliana* Mutants**	**Name/Specification of Surface Structural Mutation**	**Reference**
Col-0	*Arabidopsis thaliana* L., wild type *Columbia-0*, Family: Brassicaceae; Small flowering plant with various properties that make it an excellent model organism.	[40]
exo70H4-1	Exocyst 70H4-1 subunit/The secondary cell wall layer in trichomes is absent.	[41]
tbr1	Trichome birefringence/reduced crystalline cellulose in trichomes.	[42]
arpc5	Mutation in ARP2/3 complex subunit/Defects in the shape and adhesion of epidermal pavement cells and trichomes. Morphology with short branches.	[43]
glabra (gl1)	Few hairs occasionally on leaf margins or stems Glabra-mutation, only affects the trichome development pathway, i.e., trichomes are almost not present.	[44,45]

The studied lineages exhibit modified epidermal structure, particularly in trichome presence or trichome morphology (Table 1, Figure 1).

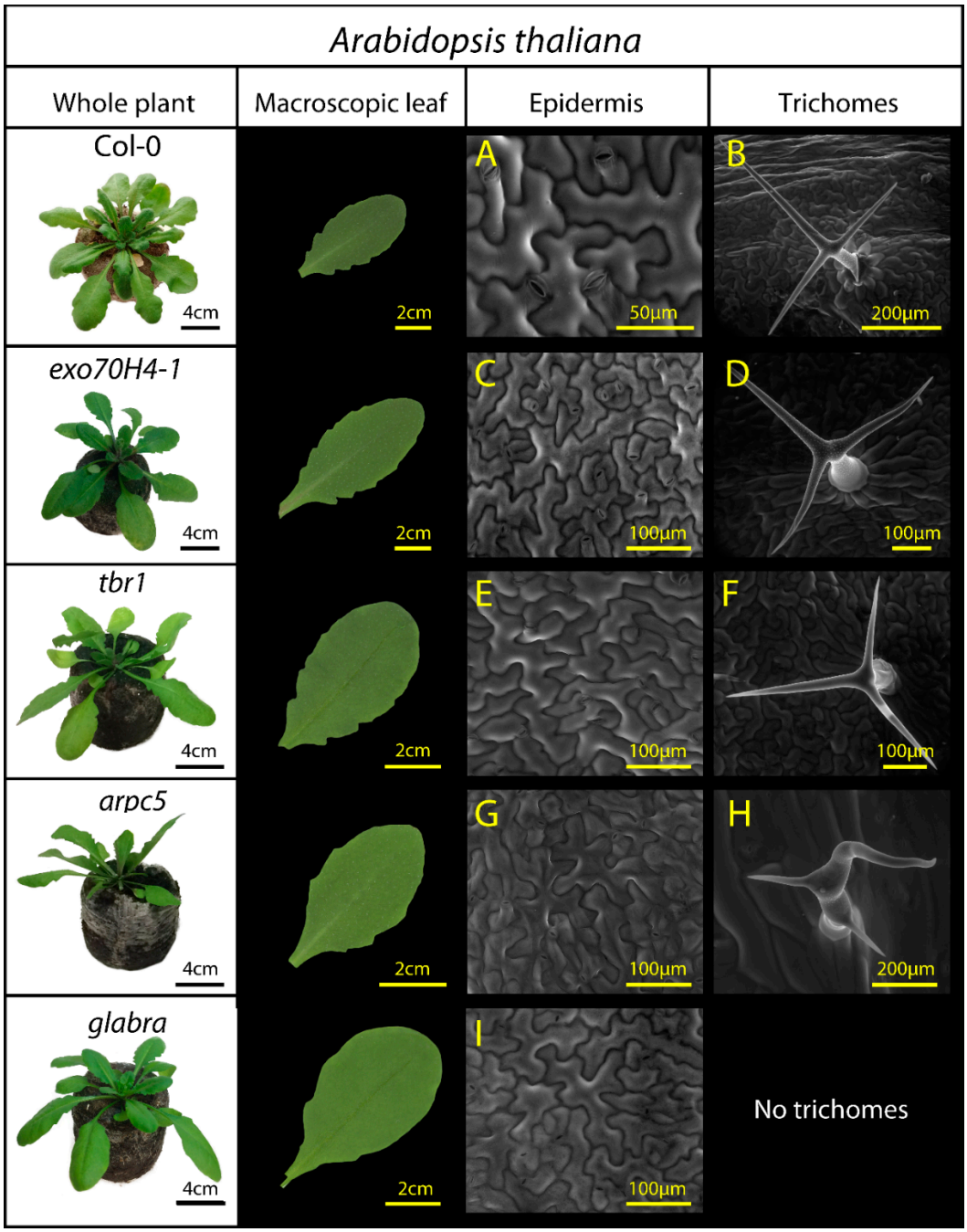


Figure 1. *A. thaliana* lineages used in the study: *Col-0* (wild type), *exo70H4-1*, *tbr1*, *arpc5*, and *glabra*. Third and fourth columns present epidermal surface observations by environmental scanning electron microscopy, including structure of pavement epidermal cells (**A**,**C**,**E**,**G**,**I**) and structure of trichomes (**B**,**D**,**F**,**H**), if present. Epidermal mutations are detailed in Table 1.

In *Arabidopsis*, the differences in epidermal properties among mutants were given by their specific genetic mutations. Apart from the *glabra* mutant, where trichomes are not observed, we expected no significant differences in trichome density, but rather in trichome structure. Distorted trichomes with short branches are characteristic of *arpc5* mutant, as is the absence of secondary cell wall in *exo70H4-1* trichomes and reduced crystalline cellulose deposition in *tbr1* trichomes.

A. thaliana plants were cultivated in a growing room with a long day (16 h light and 8 h dark (16/8)) in temperature 24 °C, with 100 µmol m^{-2} s^{-1} without any artificial

illumination, for 14 days in August 2018 to achieve suitable germination. To prevent early maturation and flowering of *A. thaliana* plants in long-day conditions, they were moved to the greenhouse without controlled temperature conditions and ambient, natural illumination and grown for the next 2 months from August to September 2018 until leaf area of their leaves was sufficient for the measurements in the integrating sphere and all biochemical and structural analyses.

In addition to the *Arabidopsis* experimental system, we selected six species of the *Hieracium* genus with differences in indumentum: *H. prenanthoides* Vill., *H. intybaceum* All., *H. sabaudum* L., *H. nigrescens* Willd., *H. setigerum* Tausch, and *H. coldei* Szeląg (Table 2).

Table 2. Leaf description including epidermal surface structure, ecology of six *Hieracium* species from a referenced study.

***Hieracium* sp.**	**Leaf Description, Including Epidermal Surface Structure**	**Species Ecology**	**Reference**
H. prenanthoides	Dark green adaxial side, lighter grey-green abaxial side. No info on trichomes available in literature.	Montane and submontane wild species, growing above timberline	[46]
H. intybaceum	Soft leaves covered with glandular trichomes that produce a sticky resinous exudate.	Alpine species sometimes considered as alpine endemite.	[47,48]
H. sabaudum	Tough leathery leaves, glabrous on adaxial side and dark green, abaxial side with scattered short trichomes.	European species growing in light deciduous and pine forests, rocky and anthropogenic stands	[49]
H. nigrescens	Hairy leaves, particularly on the abaxial side, trichomes usually localised on the midrib and petiole, short stalky trichomes on the leaf margins.	Subalpine and supramontane part of Krkonoše Mts. (Giant Mountains, Czechia), montane grasslands dominated by Nardus stricta	[50]
H. setigerum	Green-grey (waxes) leaf colour, rarely long simple scattered trichomes and branched trichomes on the adaxial leaf side, dendritically branched dense trichomes on the abaxial leaf side	Isolated stands in central and southeastern Europe, up to 1000 m a.s.l.	[46]
H. coldei	Green-grey (waxes) varying leaf colour, long simple scattered trichomes on the adaxial leaf side.	Relict habitats in crevices of andesite rock in the Harghita Mountains (East Carpathians)	[51]

These *Hieracium* species exhibit natural variation in the epidermal structure, including differences in trichome length and density, and in the epicuticular wax abundance and structure (Table 2, Figure 2). We observed three trichome morphology types in the studied *Hieracium* species: mostly glandular trichomes (*H. prenanthoides*, *H. intybaceum*, *H. sabaudum*, *H. nigrescens*, *H. coldei*), (Figure 2B,E,F,I,O), followed by stiff trichomes (*H. prenanthoides*, *H. sabaudum*, *H. nigrescens*, *H. setigerum*, *H. coldei*), (Figure 2C,G,J,M,P) and branched (stellate) trichomes (*H. setigerum*) (Figure 2L). All these differences may affect specular reflectance.

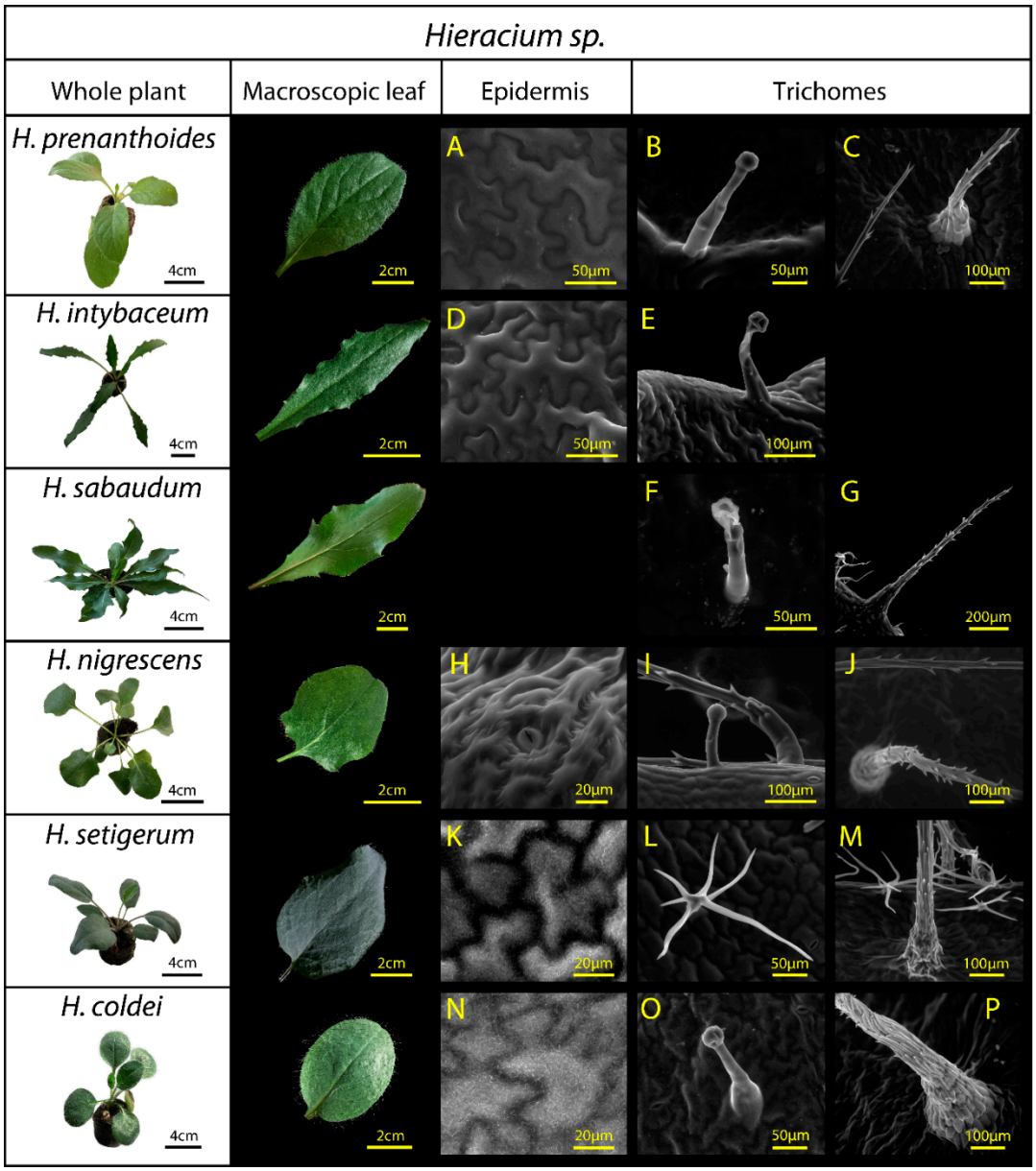


Figure 2. *Hieracium* species used in the study: *H. prenanthoides*, *H. intybaceum*, *H. sabaudum*, *H. nigrescens*, *H. setigerum*, and *H. coldei*. The three columns on the right (**A**–**P**) present epidermal surface observations by environmental scanning electron microscopy. Third column: leaf epidermal pavement cells without waxes (**A**,**D**,**H**), and with a wax layer on the epidermal pavement cells (**K**,**N**). Fourth column: glandular trichomes (**B**,**E**,**F**,**I** (a smaller one),**O**) and branched (stellate) trichome in *H. setigerum* (**L**). Fifth column: multicellular stiff trichomes (**C**,**G**,**I** (base of the trichome at right)) **J**,**M** (base of the trichome in front), **P** (base of the trichome). For expanded description of surface structures, see Table 2. Due to the epidermal cell collapsing during ESEM acquisition, we did not include *H. sabaudum* epidermal cells in the figure; however, we did not observe there any surface waxes, or roughness on the surface, which could influence leaf reflectance.

Hieracium plants were cultivated in a growing room under short-day conditions (8/16), to prevent plants from early flowering at a temperature of 24 °C, with 120 µmol m^{-2} s^{-1}, without any additional artificial illumination, for approximately 2 months from May to July 2019.

For optical measurements, we selected leaves with sufficiently large leaf area to fully cover a field of view in the integrating sphere (diameter = 1.5 cm), regardless of leaf insertion. The same leaves used for optical measurements were used also for analysing leaf structural parameters.

2.1.2. Anatomical Structure Assessment

Specific leaf area (SLA) was determined for *A. thaliana* plants and *Hieracium* species on leaves sampled during the day of harvesting. Leaves were weighed, scanned, then placed into an oven for 3 days at 60 °C. After drying, the samples were weighed again and their leaf areas were expressed as leaf area per unit of dry mass as determined using ImageJ software (https://imagej.net/ (accessed on 15 October 2021)) while following the protocol of [52,53].

Microscopic visualisation of leaf epidermal surface structures of *A. thaliana* and *Hieracium* species (including size and type of trichomes and presence of epicuticular wax deposition) was performed using a Quanta 200 Environmental Scanning Electron Microscope (ESEM), (FEI Technologies Inc. Hillsboro, Oregon 97124, USA;Thermo Fischer Scientific) up to 1 week from the day of optical properties measurements. Fresh leaves were scanned in the native state in the environmental chamber of the microscope. The specimen was observed under pressure of 260 Pa and temperature −12 °C with water equilibrium and 100% relative humidity. Quantification of trichome density for *A. thaliana* leaves was performed from scanned fresh true leaves with 600 dpi resolution while using a systematically uniform sampling approach [41] and point-counting method with superimposed point grid in ImageJ.

Quantitative anatomical analysis of trichome density was performed for *Hieracium* species on fixed leaf samples. Leaf segments (squares of 0.5 cm^2) of all samples were fixed in formalin–acetic acid–alcohol (FAA) fixative (70% ethanol, 40% formaldehyde, acetic acid in volume ratio 90:5:5). Images of fixed leaf segments stained with toluidine blue to visualise cell walls [54] were acquired by a Cannon EOS100D camera mounted on an Olympus BX40 microscope with 30× magnification. To assess trichome length and density on equal leaf area, a square mask of 12.8 mm^2 was applied on each image in AdobePhotoshop Lightroom 3.0 software (https://www.adobe.com/products/photoshop-lightroom.html (accessed on 15 October 2021)) and trichomes were counted manually in ImageJ using an unbiased counting frame.

Leaf cross sections (about 80 µm thick) of *Hieracium* leaves were prepared from previously FAA-fixed leaf samples using a hand microtome and then stained by toluidine blue [54]. Using a light microscope, bright field images (five per each leaf segment) were acquired using the same microscope and camera and processed in ImageJ to measure leaf thickness parameters [52]. These were whole leaf thickness; thicknesses of mesophyll, palisade, and spongy parenchyma; and thicknesses of adaxial (upper) and abaxial (lower) epidermis. Each parameter was measured three times on each image in leaf cross section at regular intervals. The ratio of palisade to spongy parenchyma (PP/SP) was calculated.

Based on our observation, there was no significant difference in SLA among the genotypes of *A. thaliana* with the exception that there was a significant difference between *Col-0* and *arpc5*. We decided, however, not to perform leaf sectioning.

2.2. Leaf Optical Properties Assessment

Leaf optical properties in the 350–2500 nm spectral range were measured by spectroradiometer ASD FieldSpec 4 with an integrating sphere ASD 190 RTS—3ZC (both Malvern Panalytical, Cambridge, UK [55]. This allowed us to measure hemispherical integrated reflectance as the directional–hemispherical reflectance factor (DHRF) [16] of the adaxial side of the leaf. For *Arabidopsis*, whole leaves were used for completely covering the field of view of the integrating sphere; for *Hieracium*, leaves were measured excluding the midrib region if possible. Measurements were taken in digital number (DN) values and the integration time was 136 ms, averaging 25 readings for sample measurements and 50 readings for instrument optimisation. White calibration measurements were taken after each sample, no longer than 15-minute intervals between. The sphere was specifically designed to allow specular reflectance measurements by placing a light trap in the corresponding specular reflection measurement geometry. Two reflectance quantities, in the same sample positions, can be measured: (1) total directional–hemispherical reflectance including specular

component (R_{TOT}), and (2) leaf directional–hemispherical reflectance with the specular component removed from the total reflectance (R_{SR}). The latter corresponds to diffuse reflectance measurements when the light trap is placed in the angle equal to that of the light source relative to the sample surface (Figure 3).

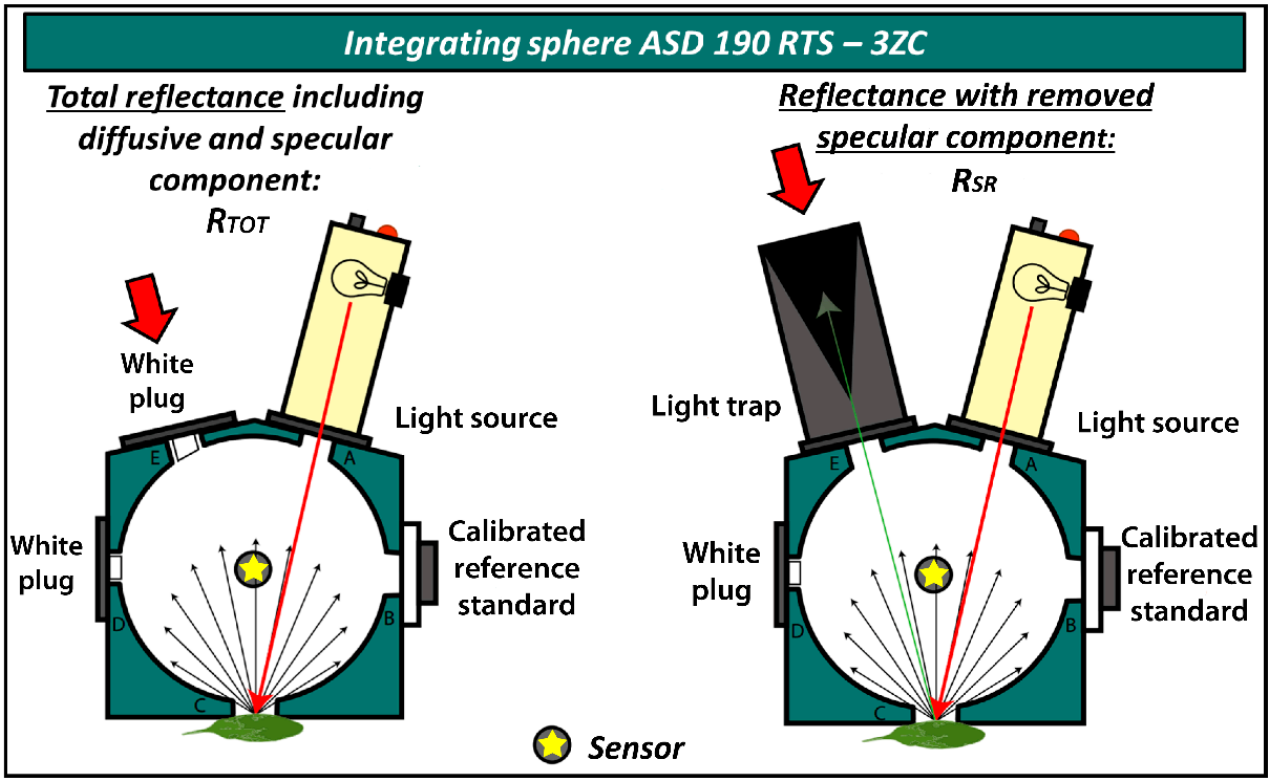


Figure 3. Measuring leaf reflectance by two integrating sphere set-ups: total reflectance (R_{TOT}) and reflectance with specular component removed (R_{SR}). Yellow star in grey circle represents the optical cable sensor, which was placed on the surface of the integrating sphere.

The specular component of reflectance (R_{SPEC}) can then be calculated as the difference R_{TOT}—R_{SR}. Due to technical problems, measurements of R_{SR} for wild type of *A. thaliana*, (*Col-0*) were not possible to accomplish. However, missing wild type (*Col-0*) used as a control in most studies on mutants is not crucial in this study. The main emphasis was put on variation in trichome density, which has been preserved even if *Col-0* was left out. For example, *tbr1* shows the same trichome density as *Col-0* (Figure 4D). In the case of *A. thaliana* lineages, spectral data were analysed only for the four mutants (*arpc5*, *exo70H4-1*, *tbr1*, and *glabra).* In total, 36 leaf samples were measured for *A. thaliana* and 45 for *Hieracium*.

2.3. Biochemical Assessment of Leaf Chlorophyll and Carotenoids Contents

After measurement of leaf optical properties by spectroradiometer, the same leaf was sampled to determine leaf pigment composition biochemically by spectrophotometer (i.e., chlorophyll a + b and total carotenoids). A leaf disc of 50 mm^2 was cut and pigments were extracted in dimethylformamide [56] until the leaf disc was bleached. Absorbances at 480 nm, 647 nm, 664 nm, and 750 nm were measured using an Evolution 201 spectrophotometer (Thermo Fisher Scientific, Waltham, MA, USA) and the contents of chlorophyll a + b (Chl a + b) and carotenoids (Car) were calculated using equations from Wellburn [57] and related to leaf area.

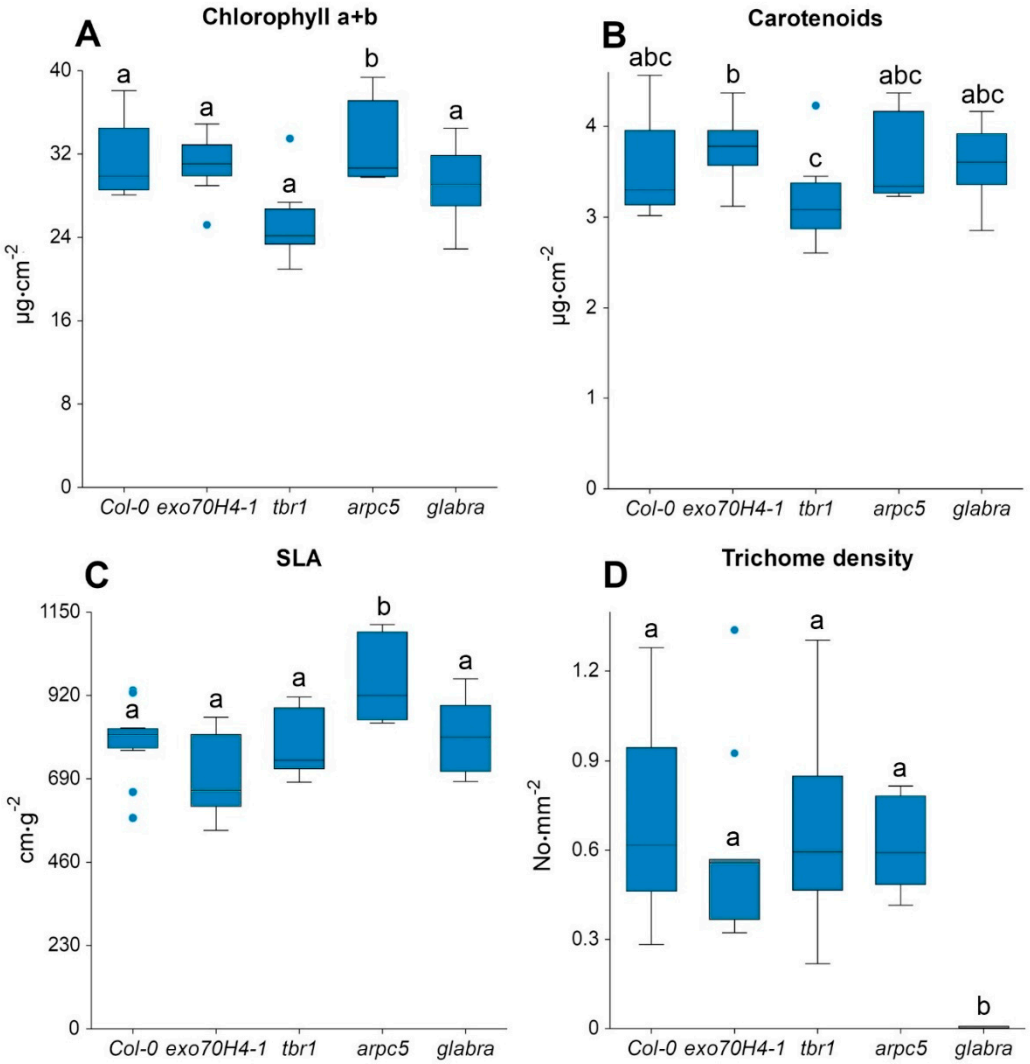


Figure 4. Leaf biochemical and structural parameters for *A. thaliana* lineages (*Col-0*, *exo70H4-1*, *tbr1*, *arpc5*, and *glabra*): (**A**) chlorophyll a + b content, (**B**) carotenoids content, (**C**) specific leaf area (SLA), and (**D**) trichome density. Differences among lineages were tested by one-way ANOVA. In the case of normal distribution, the Tukey–Kramer multiple comparison test was used; otherwise, the Kruskal–Wallis test was applied. Significance was set at a p-value < 0.05. Lines in boxes show median, bars show the inter-quartile range, and dots correspond to outliers.

2.4. Data Processing and Statistical Analysis

2.4.1. Biophysical Properties

Statistical comparison of selected leaf biochemical and structural traits (Chl a + b, Car, SLA, trichome length and density, and leaf thickness) were performed using NCSS 9 software by means of one-way ANOVA separately for *Arabidopsis* and *Hieracium* plant groups. When residuals were normally distributed, the Tukey–Kramer multiple comparison test was used. Otherwise, the Kruskal–Wallis test was applied. Significance was set at p-value < 0.05.

2.4.2. Visualisation of Spectral Curves

For each species of *Hieracium* and mutants of *Arabidopsis*, an average and standard deviation of measured total reflectance (R_{TOT}) and reflectance with removed specular component (R_{SR}) was calculated from 5 to 12 individual samples. For visualisation purposes, a Savitzky–Golay filter with 3rd degree polynomial and 21 nm frame length was applied to remove spectral noise in the data. The dataset was limited to the 400–2400 nm spectra region to exclude unreliable observations with excessive noise. The R_{TOT} and R_{SR}

of species of *Hieracium* and mutant of *Arabidopsis* were visualised as a shaded error bar with average reflectance as line and standard deviation as vertical area, and R_{SPEC} on the secondary y-axis as line. For further analysis, no filtered data were used, and to exclude noisy character of spectra below 400–450 and above 1800 nm, we used spectral ranges described below.

2.4.3. Exploring of Leaf Specular Reflectance by Using PCA

Principal component analysis (PCA) was applied on specular reflectance spectra in 450–1800 nm. PCA was based on the NIPALS algorithm [58]. To reveal patterns in specular reflectance related to the selected surface traits (trichome density for both model systems; trichome length and adaxial epidermis thickness for *Hieracium*), categorical variables (mutant or species) and gradual ranges of structural traits were used for sample grouping in PCA score plots. Trichome densities in both species and epidermal thickness in *Hieracium* were log-transformed before the analysis. For *Arabidopsis*, the trichome density was not transformed as there were zero values in *glabra* mutants. The five gradual ranges of trichome density, trichome length, and adaxial epidermis thickness were automatically created by the software Unscrambler 11 (CAMO Analytics, Oslo, Norway), and were applied as categorical variables for scores grouping of surface properties.

2.4.4. PLSR Modelling

Prediction models for selected leaf biophysical and structural traits were established, using PLSR analysis with the same NIPALS algorithm as the PCA. For each leaf trait, two models were created: the first based on R_{TOT} and the second based on R_{SR}. The model input variables were the measured leaf spectra (R_{TOT} or R_{SR} between 450 and 1800 nm) representing independent variables and the leaf biophysical and surface traits were then dependent variables. The PLSR modelling included the standard calibration and the validation stages [59,60]. To assess the model performance, a random cross-validation was conducted. The model was cross validated with random segments: five segments for *Arabidopsis* and eight segments for *Hieracium*. The models were evaluated based on the standard measures [61] such as the lowest number of factors (a measure of model robustness), the lowest root mean square error of prediction (RMSEP), %RMSR (% of root mean square error (RMSE) related to average values of parameters), and the coefficient of determination (R^2). PLSR modelling was performed in Unscrambler 11 (CAMO Analytics, Oslo, Norway). Finally, the performance of models based on R_{TOT} and R_{SR} was compared.

3. Results

3.1. Leaf Biochemical and Structural Traits

Figure 5F shows the presence and abundance of trichome types (glandular, stiff, and stellate) for each species and differences in trichome type density among the species. *H. setigerum*, with branched trichomes, showed the highest total trichome density, which was significantly higher than in other *Hieracium* species, and simultaneously the highest variance in trichome density among all studied species.

We observed a similar pattern of Chl a + b and SLA among the *Arabidopsis* lineages, with only exception for *arpc5* with significantly higher values compared to other lineages (Figure 4A,C). For Car, the only significant differences were observed between *exo70h4-1* and *tbr1* mutants (Figure 4B). Significant differences in trichome density occurred between *glabra* and the other lineages (Figure 4D), as had been expected based on the descriptions of the mutants (Table 1).

Hieracium species showed no significant differences for Car (Figure 5B) and leaf thickness (Figure 5D) whereas significant differences for Chl a + b (Figure 5A) and SLA (Figure 5C) were observed among the *Hieracium* species studied. *H. sabaudum* had the lowest Chl a + b and highest SLA values among the species, and *H. setigerum* had the highest Chl a + b and lowest SLA values.

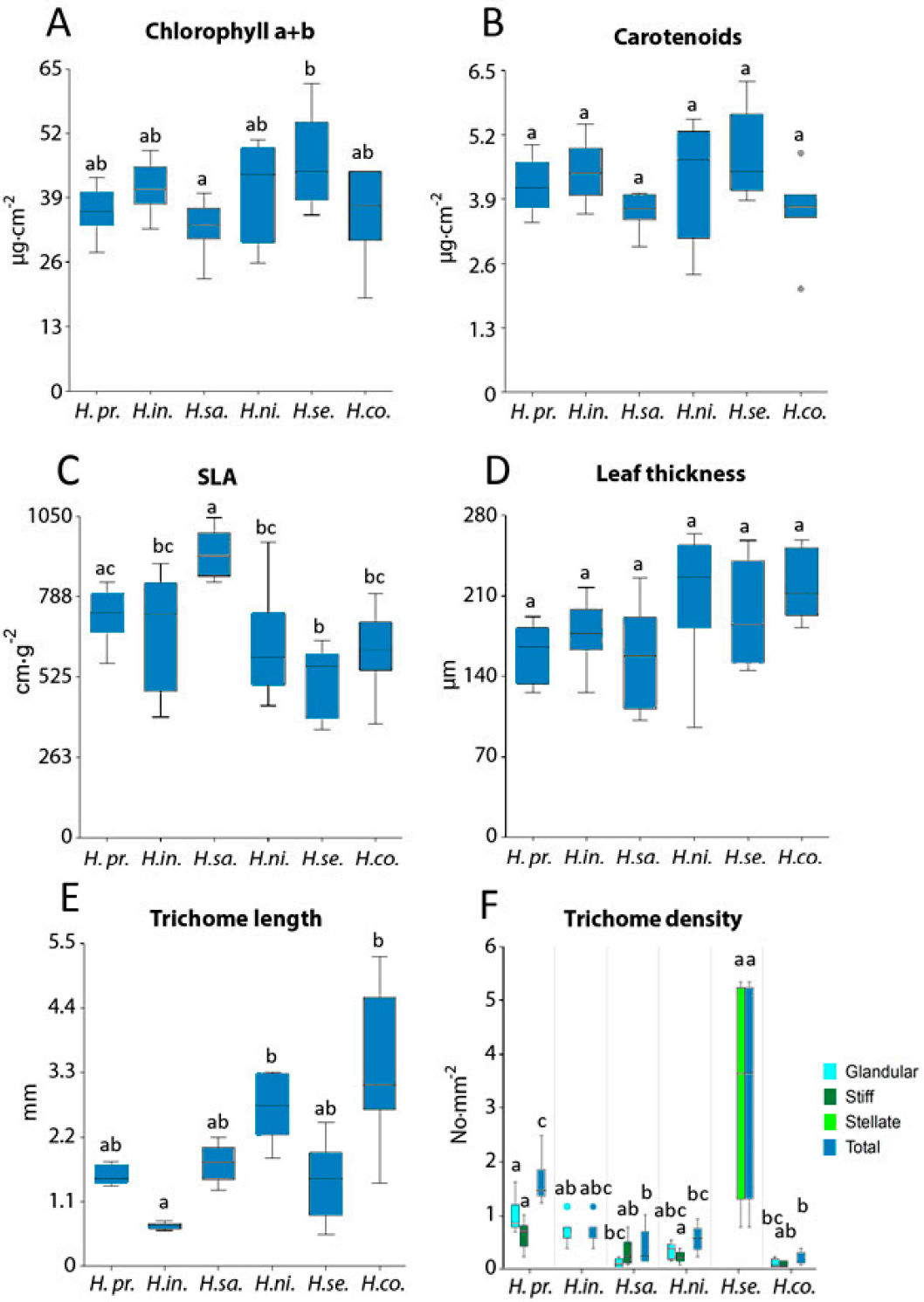


Figure 5. Leaf biochemical and structural parameters for six *Hieracium* species (*H. prenanthoides*, *H. intybaceum*, *H. sabaudum*, *H. nigrescens*, *H. setigerum*, and *H. coldei*). (**A**) Chlorophyll a + b content, (**B**) carotenoids content, (**C**) specific leaf area (SLA), (**D**) leaf thickness, (**E**) trichome length, and (**F**) trichome density. Different letters above columns correspond to statistical differences among species as tested by one-way ANOVA. In (**F**), one-way ANOVA was performed separately for each trichome type, and the only statistically significant difference in trichome density was found for stellate trichomes in comparison to glandular and stiff ones. In the case of normal distribution, the Tukey–Kramer multiple comparison test was used; otherwise, the Kruskal–Wallis test was applied. Significance was set at p-value < 0.05. Lines in boxes show median, bars show inter-quartile range; dots correspond to outliers.

In Figure 5E, we present total trichome length for *Hieracium* species regardless of the type of trichomes. In Figure 5F, we present total trichome density for *Hieracium* species with respect to the type of trichomes—glandular, stiff, and stellate—and as a total density regardless of trichome type. In case of trichome length and density, *H. coldei* had the longest stiff trichomes (up to 5 mm, Figures 2P and 5E). *H. intybaceum* (Figure 5E) had the shortest trichomes with low variance, which is given by the presence of only glandular trichomes (Figure 2E). *H. setigerum* showed the highest density of stellate (Figure 2L) trichomes compared to the rest of the *Hieracium* species with glandular or stiff trichomes (Figure 5F).

3.2. Leaf Optical Properties: Total, Diffuse, and Specular Reflectance

Leaf directional–hemispherical reflectance factor for R_{TOT} and R_{SR} (DHRF) and for specular component R_{SPEC} (R_{TOT}-R_{SR}), i.e., DHRF specular, were visualised in the spectral range 400–2400 nm (Figures 6 and 7). For individual plant mutants or species, three spectral curves, R_{TOT}, $R_{SR,}$ and R_{SPEC}, are shown in separate graphs: the average of the DHRF is marked by a solid black line for R_{TOT} and a red dashed line for R_{SR}. Grey and light red shadow areas show standard deviation belonging to the same coloured DHRF line. The blue line exhibits the average of the specular component of DHRF, R_{SPEC}.

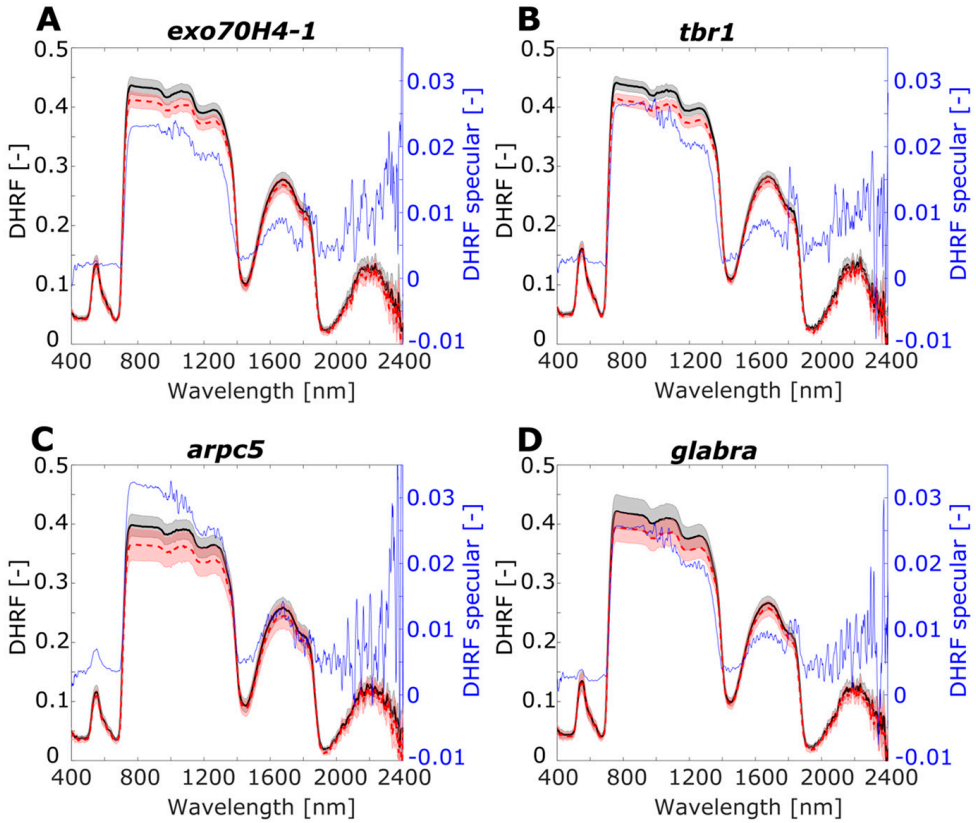


Figure 6. Leaf optical properties averaged for R_{TOT}, R_{SR}, and R_{SPEC} for *A. thaliana* lineages: (**A**) *exo70H4-1*, (**B**) *tbr1*, (**C**) *arpc5*, (**D**) *glabra*. Left y-axis shows directional–hemispherical reflectance factor (DHRF) of R_{TOT} and R_{SR}, and right y-axis corresponds to DHRF of specular component R_{SPEC}. Grey and light red shadows of R_{TOT} and for R_{SR} curves display variance among the samples by standard deviation value. Black axes (left) correspond to DHRF of R_{TOT} and R_{SR} and blue axes (right) correspond to DHRF of R_{SPEC}.

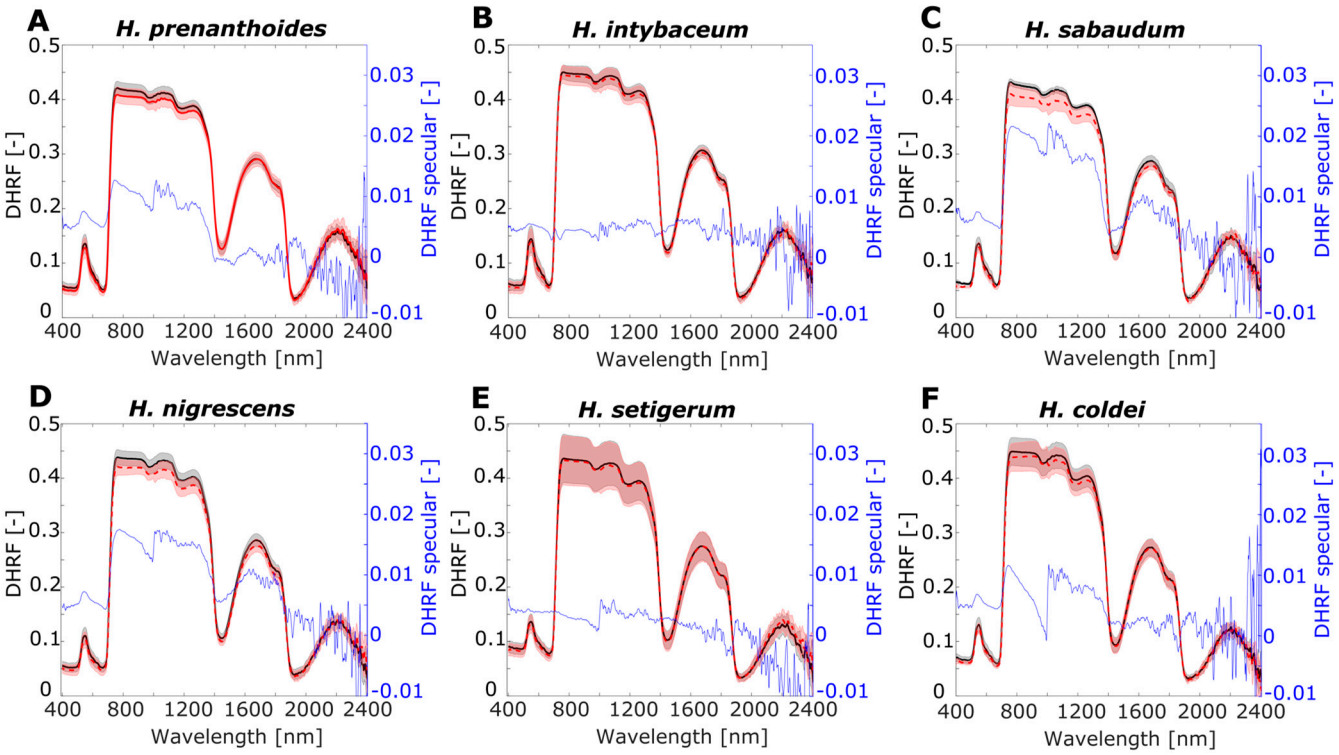


Figure 7. Leaf optical properties averaged for R_{TOT}, R_{SR}, and R_{SPEC} for *Hieracium* species (**A**) *H. prenanthoides*, (**B**) *H. intybaceum*, (**C**) *H. sabaudum*, (**D**) *H. nigrescens*, (**E**) *H. setigerum*, and (**F**) *H. coldei*. Left y-axis shows directional–hemispherical reflectance factor (DHRF) of R_{TOT} and R_{SR}, and right y-axis corresponds to DHRF of specular component R_{SPEC}. Grey and light red shadows of R_{TOT} and for R_{SR} curves display variance among the samples by standard deviation value. Black axes (left) correspond to DHRF of R_{TOT}, R_{SR} and blue axes (right) correspond to DHRF of R_{SPEC}.

For both experimental groups of plants *A. thaliana* and *Hieracium*, there was higher variance of DHFR in NIR spectral region, compared to the VIS spectral region. For the SWIR spectral region, the most pronounced variance was in the spectral interval 1500–1900 nm. The R_{TOT} and R_{SR} spectra were noisy in longer wavelengths for both groups of plants, which was also apparent for R_{SPEC}: the noise was more pronounced for *A. thaliana* than for *Hieracium*. Note that the range of R_{SPEC} is from −0.01 to 0.035 of DHRF, showing negative values due to noise only in longer SWIR wavelengths. For *A. thaliana*, R_{SPEC} is almost zero in VIS and SWIR regions, except the low green peak in *arpc5* and with higher plateau in NIR (0.025–0.03). For *Hieracium*, R_{SPEC} has no uniform pattern through the VIS, NIR, and SWIR spectral regions, and the shape of the curves differs among the species.

For all *Arabidopsis* mutants, the difference between the R_{TOT} and R_{SR} was almost negligible in VIS and R_{SR} was always lower than R_{TOT} in NIR. In NIR, *arpc5* (Figure 6C) and *glabra* (Figure 6D) showed remarkably lower R_{SR} than R_{TOT} although having quite high variance, in contrast to *exo70H4-1* and *tbr1* with low variances (Figure 6A,B). In SWIR, the difference between R_{TOT} and R_{SR} was also negligible, and this spectral region was noisy for all the mutants. The shape of the R_{SPEC} curve in NIR and SWIR up to 1700 nm had the similar shape as R_{TOT} and R_{SR}, with the highest values in NIR reaching 0.03 of DHRF. In the VIS region, only *arpc5* mutant displayed a small peak in the green spectral region (0.007 DHRF), in contrast to other three mutants, where the R_{SPEC} was almost flat.

For *Hieracium*, the difference between RSR and RTOT was negligible in VIS for all studied species (Figure 7). In NIR, *H. prenanthoides*, *H. sabaudum*, and *H. nigrescens* (Figure 7A,C,D) showed lower R_{SR} than R_{TOT} in contrast to *H. intybaceum*, *H. setigerum*, and *H. coldei* (Figure 7B,E,F) with almost no difference in R_{SR} and R_{TOT}. In SWIR, minutely lower R_{SR} than R_{TOT} were detected in *H. intybaceum*, *H. sabaudum*, and *H. nigrescens* (Figure 7B–D). In the rest of the species, R_{SR} and R_{TOT} were almost equal in the SWIR

region. R_{TOT} and R_{SR} also have the highest variance in NIR, especially *H. setigerum* and *H. coldei* (Figure 7E,F); medium variance was observed for *H. intybaceum* and *H. nigrescens* (Figure 7B,D). For *H. sabaudum*, the variance in NIR was remarkably higher for R_{SR} than for R_{TOT} (Figure 7C). R_{SPEC} is very small for *Hieracium* species and does not exhibit any pattern, except for the higher values in NIR for *H. sabaudum* and *H. nigrescens* with values of DHRF 0.02 (Figure 7C,D).

3.3. PCA of Specular Reflectance—Effect of Leaf Surface Properties

PCA was applied on specular reflectance in the 450–1800 nm spectral range in both plant model systems, *A. thaliana* and *Hieracium*, to reveal R_{SPEC} relation to trichome density and length. To find a common pattern of structure in spectral data, we first grouped the scores according to mutants (in *A. thaliana*) or species (in *Hieracium*). Despite the significant differences in trichome density in both model plant lineages and trichome length in *Hieracium* confirmed by the ANOVA analysis (Figures 3 and 4), there was not any apparent clustering linked to mutant or species categories (data not shown). As there was a considerable variation in epidermal traits, we designed five gradual ranges of trichome density, trichome length, and adaxial epidermis thickness which were applied as categorical variables for scores grouping. Figure 8 shows score plots of PCA applied on specular reflectance between 450 and 1800 nm. Different colours and shapes correspond to five intervals of studied epidermal surface traits. As the representatives for all five intervals are distributed evenly along the PC1 and PC2 coordinate space, we conclude that there is no systematic relationship of R_{SPEC} to trichome density in studied *A. thaliana* lineages and *Hieracium* species, similarly as for trichome length and adaxial epidermal thickness in *Hieracium*.

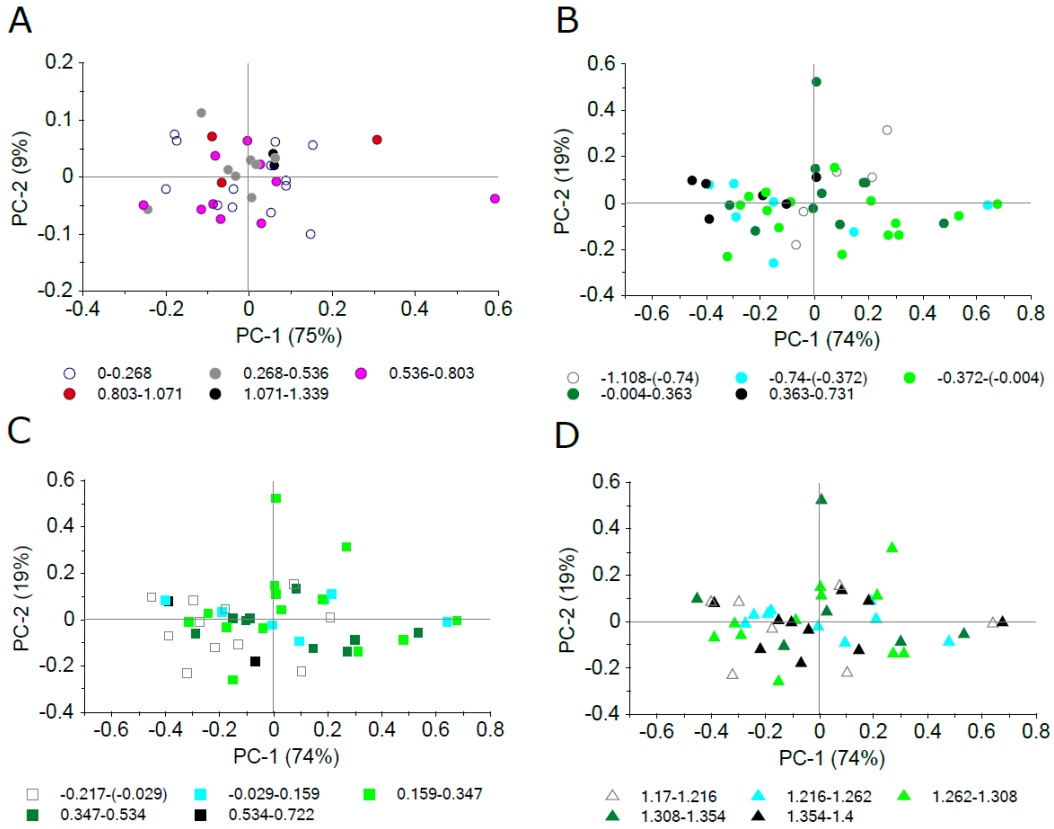


Figure 8. Principal component analysis of specular reflectance in 450–1800 nm. Sample scores are grouped into five gradual intervals of surface properties, which were automatically created by the software Unscrambler 11 (CAMO Analytics, Oslo, Norway). (**A**) *A. thaliana* trichome density, (**B**) *Hieracium* sp. trichome density (log-transformed), (**C**) *Hieracium* sp. trichome length (log-transformed), (**D**) *Hieracium* sp. adaxial epidermis thickness (log-transformed).

3.4. Predicting Leaf Biochemical and Structural Traits by PLSR Models

We hypothesised that the exclusion of leaf specular reflectance would improve the performance of PLSR models for leaf biochemical traits estimation, as the specular reflectance does not origin from the leaf interior. The results of PLSR models based on R_{TOT} and R_{SR} for prediction of biophysical and structural traits of *A. thaliana* mutants and *Hieracium* species are given in Table 3.

Table 3. Parameters of calibration and validation of PLSR models based on R_{TOT} and R_{SR} spectra between 450–1800 nm, for *A. thaliana* mutants and *Hieracium* sp. for biophysical traits. Left side of the table represents calibration and validation of PLSR models based on R_{TOT} spectra and right side of the table represents models based on R_{SR}. Columns represent: Factors (number of components used in model creation), RMSE (root mean square error), RMSE% (% of RMSE related to average values of parameters), R2 (Coefficient of determination) of calibration and validation of models.

	R_{TOT}							**R_{SR}**						
	Calibration				Validation			Calibration				Validation		
	Factors	RMSE	RMSE%	R^2	RMSE	RMSE%	R^2	Factors	RMSE	RMSE%	R^2	RMSE	RMSE%	R^2
Arabidopsis														
Chlorophyll a + b	4	1.07	3.65	0.93	1.62	5.52	0.85	3	1.37	4.67	0.88	1.69	5.76	0.83
Carotenoids	3	0.23	6.47	0.72	0.27	7.59	0.64	3	0.22	6.19	0.74	0.26	7.31	0.70
SLA	6	38.88	4.93	0.91	110.58	14.02	0.27	5	52.88	6.70	0.83	98.35	12.47	0.46
DW/FW	4	0.01	11.47	0.65	0.01	11.47	0.47	4	0.01	11.47	0.66	0.01	11.47	0.50
Trichome density	1	0.35	84.17	0.10	0.37	88.98	0.02	5	0.16	38.48	0.79	0.35	84.17	0.12
Hieracium														
Chlorophyll a + b	4	6.45	16.38	0.39	7.34	18.64	0.23	4	5.94	15.09	0.48	7.04	17.88	0.32
Carotenoids	4	0.72	16.99	0.28	0.80	18.87	0.15	4	0.66	15.57	0.39	0.74	17.46	0.24
SLA	5	74.29	11.09	0.82	103.30	15.42	0.66	5	69.00	10.30	0.84	91.79	13.70	0.73
DW/FW	5	0.01	10.44	0.79	0.01	10.44	0.67	5	0.01	10.44	0.82	0.01	10.44	0.74
Trichome density	4	0.82	54.85	0.55	0.97	64.89	0.42	4	0.78	52.18	0.59	0.93	62.21	0.43
Leaf thickness	3	28.62	15.37	0.57	30.59	16.43	0.53	3	29.58	15.89	0.54	32.55	17.48	0.45
Palisade parench.	4	14.93	24.74	0.63	17.45	28.91	0.53	4	14.44	23.93	0.65	16.90	28.00	0.57
Spongy parench.	5	16.75	22.52	0.75	20.61	27.71	0.63	4	18.39	24.73	0.70	21.85	29.38	0.58
Trichome length	2	0.73	39.97	0.37	0.84	45.99	0.16	2	0.74	40.52	0.35	0.90	49.28	0.10

The evaluation of model performances was based on the following parameters: R^2, RMSE, %RMSE, and the number of factors explaining the variability of a modelled trait. In the case of *A. thaliana*, only biophysical traits (chlorophyll and carotenoids contents SLA, DW) and trichome density were modelled (Table 3); for *Hieracium*, we present prediction models for both biophysical and anatomical traits (Table 3). These include trichome density and length, leaf thickness, and thicknesses of palisade and spongy parenchyma.

When comparing the *A. thaliana* and *Hieracium* PLSR models, the prediction of leaf biochemical pigments (Chl a + b, Car) and SLA performed better for *A. thaliana* than for *Hieracium* sp. In contrast, the model calibration for leaf anatomical properties prediction was better for *Hieracium* sp. than for the *Arabidopsis* group. The model validations show slightly better results for *A. thaliana* models based on R_{TOT} than for R_{SR}. In *Hieracium*, the validations are better for models based on R_{SR} than for R_{TOT}.

The effect of specular reflectance removal on PLSR model performance in *A. thaliana* was neutral or slightly negative in comparison to models based on R_{TOT}. In *A. thaliana*, the most remarkable difference between PLSR models based on R_{TOT} and R_{SR} was for SLA, where the model was better for R_{TOT} than for R_{SR}. In *Hieracium*, the effect of removing specular reflectance had both positive and negative effects on models; however, neither the improving nor the worsening of the model performance was considerable.

4. Discussion

Several authors [36,39] have studied species with and without trichomes in relation to their leaf reflectance; however, investigations of the relationship between reflectance and quantitative epidermal parameters—trichome length and density quantification—are missing in the literature. We discuss the results of our investigation as follows: in

Section 4.1, we focus on variation in biochemical and surface structural leaf traits to confirm our assumption about the variability of these traits in plant model systems. In Section 4.2, we address our first hypothesis (i.e., that epidermal traits affect the specular reflectance and that leaves with denser and longer trichomes have lower specular and higher total reflectance) and we discuss the relation of leaf specular reflectance to its surface properties. Finally, in Section 4.3, we evaluate how the specular reflectance removal affects PLSR modelling of biophysical traits.

4.1. Structural and Biochemical Parameters Variation

4.1.1. Trichome Density

Variation in trichome morphology in *A. thaliana* mutants and *Hieracium* species were confirmed qualitatively via ESEM images (Figures 1 and 2, respectively). Moreover, quantitative differences were detected in total trichome density for *A. thaliana* and in density of trichome among the species of *Hieracium* (Figure 5F). In *Arabidopsis*, it is known that the trichome distribution on the leaf surface corresponds to its vegetative phase (juvenile, adult; [62]) and also depends on leaf insertion. In the present study, measurements of leaf optical properties in *Arabidopsis* were conducted on mature vegetative leaves so that the size of the leaf would fit the field of a view of the integrating sphere. Our *A. thaliana* leaves exhibited relatively low trichome density of 0–1.2 mm^{-2} in comparison to the range of 0.3–3.84 trichomes mm^{-2} observed in 26 *A. thaliana* ecotypes [63]. We emphasise that the trichome quantitative and qualitative descriptions presented in Figure 2 correspond to mature vegetative leaves of ontogenetically relatively young *Hieracium* individuals sampled at the time of measuring the leaf optical properties and sampling for ESEM analysis. The trichome densities in *Hieracium* leaves (0.2–5.5 mm^{-2} on average) are also rather low in comparison with literature—e.g., 15.4 trichomes mm^{-2} in *H. albiflorum* [64]—which, however, was not included in our study.

4.1.2. Ecophysiological Function of Leaf Surface

The selected *Hieracium* species are adapted to mountain environments (see references in Table 1), where the trichomes play an important role in reflecting excessive UV radiation, increasing the leaf boundary layer, and preventing leaf overheating. Similar protection is provided by leaf surface waxes, but, in contrast to leaf trichomes, the waxes have already been shown to increase the specular component of reflectance [34]. Due to the common genus and habitat of all the studied *Hieracium* species, there is a similarity in trichome composition in terms of morphology and density (except that the *H. setigerum* is adapted to a drier environment) and leaf thicknesses [65]. The *Hieracium* genus is known for its ability to hybridise among the species [66], and differences in trichome parameters are often observed [67]. We selected this genus to take advantage of such a variation in trichome parameters.

4.1.3. Leaf Biochemical Traits

The biochemical traits studied (chlorophyll a + b and carotenoids) exhibited small variability in both *A. thaliana* (Figure 4A,B) and *Hieracium* (Figure 5A,B). This was in accordance with the macroscopic plant homogeneity, stable cultivation conditions, and absence of stress factors. Differences in leaf chlorophyll content and SLA (Figure 5A,C) showed inverse trends among the *Hieracium* species, which corresponds to their adaptation to a specific environment or species area occurrence. Based on our study, mountain or foothill species (*H. prenanthoides*, *H. intybaceum*, *H. nigrescens*, and *H. coldei*) with similar ecology (see Table 1) also did not differ in either chlorophyll a + b content or SLA. Leaves of *H. sabaudum* showed greater SLA, indicating a lower density of mesophyll tissue and low chlorophyll a + b content, corresponding to their adaptation for growth in forest understory. Waxy leaves (Figure 2K,N) of *H. setigerum* with frequently branched, stellate trichomes (Figure 2L) contained high chlorophyll a + b content and low SLA, thus indi-

cating a trend towards more xeromorphic adaptation to fit the conditions of south and south-eastern Europe.

4.2. Optical Properties Related to Leaf Surface Traits

Previous studies [36,68,69] have described that hairy leaves reflect more light in VIS compared to leaves without trichomes. We did not confirm this observation on *Arabidopsis*, as the green peak of VIS reflectance of the *glabra* mutant (hairless lineage) was very similar to *exo70H4-1* and slightly higher than *arpc5*, both lineages bearing trichomes (Figure 6). We explain this contradiction by the fact that the studies cited above focused on leaves with high density of trichomes such as *Artemisia tridentata* and *Salix commutata* (very hairy leaves), comparing them with, e.g., *Populus tremuloides* and *Salix lemmonii* (smooth leaves) [68].

A study of Mershon et al. [70] suggests that trichome morphology rather than density affects leaf reflectance. Those authors showed that a presence of dendritic trichomes resulted in greater reflectance in the VIS spectral region compared to the effect of simple trichomes. Our results point to a similar trend, as *H. setigerum*, the only species having branched (stellate) trichomes among the *Hieracium* genus (Figure 2L), showed the highest reflectance values (both total and diffuse) in blue and red parts of the VIS spectral region in comparison to the other *Hieracium* species having only stiff and glandular trichomes (Figure 7E). However, the PCA did not reveal species clustering based on trichome morphology.

Spectral measurements of both studied groups of plants, *A. thaliana* mutants and *Hieracium* species, confirmed the assumption [8] that exclusion of R_{SPEC} from R_{TOT} decreases DHRF in the 400–2400 nm range (Figures 6 and 7). Numerous studies [8,13,26,34] indicate that smooth leaves have higher ratios of R_{SPEC} to R_{SR} than leaves with trichomes. *A. thaliana*, which had lower trichome density than *Hieracium*, showed noticeably higher R_{SPEC} in NIR (Figures 6 and 7). The effect of trichomes on leaf optical properties is the most obvious in *H. setigerum* with the highest trichome density and the biggest variance in R_{TOT} and R_{SR} in NIR accompanied by almost zero R_{SPEC}. We tested the potential of R_{SPEC} to optically distinguish plants according to their trichome density and length using PCA (Figure 8). We reject the hypothesis that the leaves with denser and longer trichomes we studied have lower specular reflectance than the smooth leaves with fewer or no trichomes. We agree with [15] that specular reflectance does not serve for prediction about trichome density. The authors of [27] demonstrated that glossy leaves have the sharpest peak of bidirectional reflectance distribution function in the specular direction (i.e., the highest R_{SPEC} in our measurement approach) compared to rarely or densely haired leaves. None of the model plants used in the present study had apparently glossy leaves and it seems plausible that the gradient in leaf surface properties was insufficient to reveal the above-cited effects of epidermal structure on specular reflection.

Qiu et al. [26] estimated that surface reflectance, and particularly its specular component, is predominantly driven by thick cuticle and heavy wax cover, but none of our studied plants exhibited these highly xeromorphic leaf traits. The only two *Hieracium* species showing indistinctive, rather smooth waxy structures on ESEM were *H. setigerum* and *H. coldei* (Figure 2K,N); however, the effect of waxes was nevertheless weak, as we did not detect lower R_{SR} in their cases in comparison to the other studied species.

4.3. PLSR Modelling of Structural and Biochemical Traits

Spectral-based estimation of chlorophyll a + b and carotenoids contents depends on optical information from the leaf interior, and the specular component could, as previously hypothesised [18], bring additional noise to the spectral signal. Grant [8] showed that exclusion of the specular component from total reflectance could successfully be used to improve chlorophyll retrieval from leaf optical properties. In *Hieracium*, we achieved very slight improvement in PLSR model performance after the specular reflectance was removed in most biophysical parameters (except for leaf thickness, spongy parenchyma

thickness, and trichome length). However, these improvements were less than 2% of RMSE. In *A. thaliana*, the effect of IS setup on the PLSR models' performance was almost negligible and rather random. Bell and Curran [71] observed that the exclusion of specular reflectance improved correlation at the canopy level between leaf area, fresh and dry weights, and optical properties in VIS spectral region more so than in NIR. We tested PLSR models based on R_{SR} and R_{TOT} at the leaf level, which involved continual spectrum from 450 to 1800 nm, and we achieved subtle improvement of models for SLA and FW/DW ratio only in *Hieracium*, not in *A. thaliana.* This finding is rather surprising because *A. thaliana* had higher R_{SPEC} than *Hieracium*, thus more significant model improvement could have been expected. Due to the very small differences in model performance based on R_{SR} compared to R_{TOT}, we cannot confirm that specular reflectance removal can significantly improve biophysical traits prediction in herbaceous dorsiventral leaves with relatively sparse trichomes of various morphology and without apparent pronounced waxy surface causing leaf surface roughness.

Although specular reflectance may not affect biophysical parameters' retrieval in sparsely hairy leaves such as the leaves analysed in the present study, it is worth considering it in radiative transfer modelling (RTM). Difficulties in estimating chlorophyll content in plants with extremely high surface reflectance in RTM PROSPECT were previously confirmed, and chlorophyll retrieval was improved after incorporating "leaf surface reflectance parameter" (which is the difference between the refractive indices of leaf surface and interior layers) in RTM PROSPECT-Rsurf [26]. Systematic quantification of leaf surface parameters such as trichome branching, length, and density, but also wax structure, wax patterns, and cuticle thickness, could help to characterise the refractive indices of the additional surface layer incorporated by Qiu et al. [26] into radiative transfer models such as PROSPECT-Rsurf.

5. Conclusions

The measurement of specular reflectance using an integrating sphere with an additional light trap appeared to be well-suited for research on specular reflectance and its effect on biophysical and structural traits retrieval at the leaf level. We confirmed our assumptions on differences in trichome morphology (ESEM imaging) and on trichome length, density, and biophysical leaf traits (quantitative microscopic assay, biochemistry) on our two model plant systems—*A. thaliana* trichome structural mutants and various *Hieracium* species. However, PCA applied to the spectra did not reveal any systematic effect of trichome density, length, or morphology on specular reflectance between 450 and 1800 nm. Our results do not support the hypothesis that leaves with denser and longer trichomes such as those analysed in our study have lower specular and higher total reflectance than the smooth leaves.

PLSR models for the prediction of selected biophysical and structural traits were successfully constructed. Their performance was compared for models based on the total reflectance and reflectance after specular component removal. Contrastingly to our expectations, the removal of specular reflectance did not remarkably improve PLSR models—the best improvements were only up to 2% of RMSE. Therefore, we cannot draw a clear conclusion regarding the effect of specular component removal on performance of PLSR models for estimation of herbaceous dorsiventral leaves with relatively sparse trichomes of various morphology and without apparent waxy surface based on a set of plant material selected for this study.

To minimise the variation in leaf traits other than epidermal surface structure, the study was conducted on closely related taxonomic units (one species *A. thaliana* and one genus *Hieracium*), which probably resulted in a too narrow range of quantitative epidermal traits than expected. However, we are convinced that specular reflectance should be further explored in plant model systems including glossy leaves and a broader gradient in trichome parameters but similar internal leaf structure. Measurements of specular reflectance using an integrating sphere with a light trap in the specular direction is possible only at the leaf

level. To reveal effects of specular reflectance on biophysical traits' retrieval at the canopy level, leaf surface parameters such as trichome branching, length, and density, as well as wax structure, wax patterns, and cuticle thickness could be incorporated into radiative transfer models.

Author Contributions: Conceptualisation, P.L., E.N., Z.L. and J.A.; methodology, E.N., P.L. and Z.L.; software, E.N., P.L. and Z.L.; data curation, E.N., P.L. and Z.L.; writing—original draft preparation, E.N., Z.L., P.L. and J.A.; writing—review and editing, E.N., Z.L., P.L. and J.A. All authors have read and agreed to the published version of the manuscript.

Funding: This research was funded by the Charles University Grant Agency (GAUK), 1752218, and partly in initial experimental phases by the NPUI LO1417 project of the Ministry of Education, Youth and Sports of the Czech Republic.

Institutional Review Board Statement: Not Applicable.

Informed Consent Statement: Not Applicable.

Data Availability Statement: The data presented in this study are available on reasonable request from the corresponding author.

Acknowledgments: We thank Ing. Jiří Machač, from the Institute of Botany of the Czech Academy of Sciences, for the environmental scanning electron microscopy image acquisition; Kateřina Schwarzerová and Petra Cifrová from the Department of Experimental Plant Biology at Charles University for precious advice regarding *Arabidopsis* cultivation; Jan Pinc, from the Department of Botany at Charles University, for the *Hieracium* seeds; for proof-reading of the paper by a native speaker, Lena Hunt from the USA, who is a student of J. Albrechtová; and Miroslav Barták for graphical technical help.

Conflicts of Interest: The authors declare that the research was conducted in the absence of any commercial or financial relationships that could be construed as a potential conflict of interest.

References

1. Ustin, S.L.; Gitelson, A.A.; Jacquemoud, S.; Schaepman, M.; Asner, G.P.; Gamon, J.A.; Zarco-Tejada, P. Retrieval of Foliar Information about Plant Pigment Systems from High Resolution Spectroscopy. *Remote Sens. Environ.* **2009**, *113*, S67–S77. [CrossRef]
2. Flood, P.J.; Kruijer, W.; Schnabel, S.K.; van der Schoor, R.; Jalink, H.; Snel, J.F.H.; Harbinson, J.; Aarts, M.G.M. Phenomics for Photosynthesis, Growth and Reflectance in Arabidopsis Thaliana Reveals Circadian and Long-Term Fluctuations in Heritability. *Plant Methods* **2016**, *12*, 1–14. [CrossRef]
3. Cotrozzi, L.; Peron, R.; Tuinstra, M.R.; Mickelbart, M.V.; Couture, J.J. Spectral Phenotyping of Physiological and Anatomical Leaf Traits Related with Maize Water Status. *Plant Physiol.* **2020**, *184*, 1363–1377. [CrossRef] [PubMed]
4. Nicodemus, F.E.; Richmond, J.C.; Hsia, J.J. *Geometrical Considerations and Nomenclature for Reflectance*; Institute for Basic Standards, National Bureau of Standards: Washington, DC, USA, 1977.
5. Jacquemoud, S.; Ustin, S. *Leaf Optical Properties*; Cambridge University Press: Cambridge, UK, 2019; ISBN 978-1-108-48126-7.
6. Breece, H.T.; Holmes, R.A. Bidirectional Scattering Characteristics of Healthy Green Soybean and Corn Leaves in Vivo. *Appl. Opt.* **1971**, *10*, 119. [CrossRef]
7. Gates, D.M.; Keegan, H.J.; Schleter, J.C.; Weidner, V.R. Spectral Properties of Plants. *Appl. Opt.* **1965**, *4*, 11–20. [CrossRef]
8. Grant, L. Diffuse and Specular Characteristics of Leaf Reflectance. *Remote Sens. Environ.* **1987**, *22*, 309–322. [CrossRef]
9. Kokaly, R.F.; Asner, G.P.; Ollinger, S.V.; Martin, M.E.; Wessman, C.A. Characterizing Canopy Biochemistry from Imaging Spectroscopy and Its Application to Ecosystem Studies. *Remote Sens. Environ.* **2009**, *113*, S78–S91. [CrossRef]
10. Allen, W.A.; Gausman, H.W.; Richardson, A.J. Willstätter-Stoll Theory of Leaf Reflectance Evaluated by Ray Tracing. *Appl. Opt. AO* **1973**, *12*, 2448–2453. [CrossRef]
11. Xiao, Y.; Tholen, D.; Zhu, X.-G. The Influence of Leaf Anatomy on the Internal Light Environment and Photosynthetic Electron Transport Rate: Exploration with a New Leaf Ray Tracing Model. *J. Exp. Bot.* **2016**, *67*, 6021–6035. [CrossRef]
12. Sinclair, T.R.; Schreiber, M.M.; Hoffer, R.M. Diffuse Reflectance Hypothesis for the Pathway of Solar Radiation Through Leaves1. *Agron. J.* **1973**, *65*, 276–283. [CrossRef]
13. Vanderbilt, V.C.; Grant, L.; Daughtry, C.S.T. Polarization of Light Scattered by Vegetation. *Proc. IEEE* **1985**, *73*, 1012–1024. [CrossRef]
14. Greiner, M.A.; Duncan, B.D.; Dierking, M.P. Bidirectional Scattering Distribution Functions of Maple and Cottonwood Leaves. *Appl. Opt.* **2007**, *46*, 6485. [CrossRef] [PubMed]
15. Grant, L.; Daughtry, C.S.T.; Vanderbilt, V.C. Polarized and Specular Reflectance Variation with Leaf Surface Features. *Physiol. Plant.* **1993**, *88*, 1–9. [CrossRef]

16. Schaepman-Strub, G.; Schaepman, M.E.; Painter, T.H.; Dangel, S.; Martonchik, J.V. Reflectance Quantities in Optical Remote Sensing—Definitions and Case Studies. *Remote Sens. Environ.* **2006**, *103*, 27–42. [CrossRef]
17. Brakke, T.W.; Smith, J.A.; Harnden, J.M. Bidirectional Scattering of Light from Tree Leaves. *Remote Sens. Environ.* **1989**, *29*, 175–183. [CrossRef]
18. Li, Y.; Chen, Y.; Huang, J. An Approach to Improve Leaf Pigment Content Retrieval by Removing Specular Reflectance Through Polarization Measurements. *IEEE Trans. Geosci. Remote Sens.* **2019**, *57*, 2173–2186. [CrossRef]
19. Vanderbilt, V.C.; Grant, L. Polarization Photometer to Measure Bidirectional Reflectance Factor R(55°, 0°; 55°,180°) of Leaves. *Opt. Eng.* **1986**, *24*, 566–571. [CrossRef]
20. McClendon, J.H. The Micro-Optics of Leaves. I. Patterns of Reflection from the Epidermis. *Am. J. Bot.* **1984**, *71*, 1391–1397. [CrossRef]
21. ASD Inc. Integrating Sphere User Manual. Available online: https://www.mapping-solutions.co.uk/downloads/data/ASD/Accessories_Brochure/A1A15.pdf (accessed on 15 October 2021).
22. Datt, B. Remote Sensing of Chlorophyll a, Chlorophyll b, Chlorophyll A+ b, and Total Carotenoid Content in Eucalyptus Leaves. *Remote Sens. Environ.* **1998**, *66*, 111–121. [CrossRef]
23. Datt, B. A New Reflectance Index for Remote Sensing of Chlorophyll Content in Higher Plants: Tests Using Eucalyptus Leaves. *J. Plant Physiol.* **1999**, *154*, 30–36. [CrossRef]
24. Sims, D.A.; Gamon, J.A. Relationships between Leaf Pigment Content and Spectral Reflectance across a Wide Range of Species, Leaf Structures and Developmental Stages. *Remote Sens. Environ.* **2002**, *81*, 337–354. [CrossRef]
25. Jay, S.; Bendoula, R.; Hadoux, X.; Féret, J.-B.; Gorretta, N. A Physically-Based Model for Retrieving Foliar Biochemistry and Leaf Orientation Using Close-Range Imaging Spectroscopy. *Remote Sens. Environ.* **2016**, *177*, 220–236. [CrossRef]
26. Qiu, F.; Chen, J.; Croft, H.; Li, J.; Zhang, Q. Retrieving Leaf Chlorophyll Content by Incorporating Variable Leaf Surface Reflectance in the PROSPECT Model. *Remote Sens.* **2019**, *11*, 1572. [CrossRef]
27. Bousquet, L.; Lachérade, S.; Jacquemoud, S.; Moya, I. Leaf BRDF Measurements and Model for Specular and Diffuse Components Differentiation. *Remote Sens. Environ.* **2005**, *98*, 201–211. [CrossRef]
28. Vogelmann, T.C.; Gorton, H.L. Leaf: Light Capture in the Photosynthetic Organ. In *The Structural Basis of Biological Energy Generation*; Springer: Berlin/Heidelberg, Germany, 2014.
29. Woolley, J.T. Reflectance and Transmittance of Light by Leaves. *Plant Physiol.* **1971**, *47*, 656–662. [CrossRef] [PubMed]
30. Li, W.; Sun, Z.; Lu, S.; Omasa, K. Estimation of the Leaf Chlorophyll Content Using Multiangular Spectral Reflectance Factor. *Plant Cell Environ.* **2019**, *42*, 3152–3165. [CrossRef]
31. Berry, Z.C.; Goldsmith, G.R. Diffuse Light and Wetting Differentially Affect Tropical Tree Leaf Photosynthesis. *New Phytol.* **2020**, *225*, 143–153. [CrossRef]
32. Vanderbilt, V.C.; Grant, L.; Biehl, L.L.; Robinson, B.F. Specular, Diffuse, and Polarized Light Scattered by Two Wheat Canopies. *Appl. Opt.* **1985**, *24*, 2408. [CrossRef]
33. Smith, W.K.; McClean, T.M. Adaptive Relationship Between Leaf Water Repellency, Stomatal Distribution, and Gas Exchange. *Am. J. Bot.* **1989**, *76*, 465–469. [CrossRef]
34. van de Kerkhof, G.T.; Schertel, L.; Poon, R.; Jacucci, G.; Glover, B.J.; Vignolini, S. Disordered Wax Platelets on Tradescantia Pallida Leaves Create Golden Shine. *Faraday Discuss.* **2020**, *223*, 207–215. [CrossRef]
35. Gates, D.M.; Tantraporn, W. The Reflectivity of Deciduous Trees and Herbaceous Plants in the Infrared to 25 Microns. *Science* **1952**, *115*, 613–616. [CrossRef] [PubMed]
36. Holmes, M.G.; Keiller, D.R. Effects of Pubescence and Waxes on the Reflectance of Leaves in the Ultraviolet and Photosynthetic Wavebands: A Comparison of a Range of Species: Ultraviolet Leaf Reflectance. *Plant Cell Environ.* **2002**, *25*, 85–93. [CrossRef]
37. Gausman, H.W.; Cardenas, R. Effect of Leaf Pubescence of Gynura Aurantiaca on Light Reflectance. *Bot. Gaz.* **1969**, *130*, 158–162. [CrossRef]
38. Levizou, E.; Drilias, P.; Psaras, G.K.; Manetas, Y. Nondestructive Assessment of Leaf Chemistry and Physiology through Spectral Reflectance Measurements May Be Misleading When Changes in Trichome Density Co-Occur. *New Phytol.* **2005**, *165*, 463–472. [CrossRef]
39. Buschmann, C.; Lenk, S.; Lichtenthaler, H.K. Reflectance Spectra and Images of Green Leaves with Different Tissue Structure and Chlorophyll Content. *Isr. J. Plant Sci.* **2012**, *60*, 49–64. [CrossRef]
40. Meyerowitz, E.M.; Pruitt, R.E. Arabidopsis Thaliana and Plant Molecular Genetics. *Sci. New Ser.* **1985**, *229*, 1214–1218. [CrossRef]
41. Kulich, I.; Vojtíková, Z.; Glanc, M.; Ortmannová, J.; Rasmann, S.; Žárský, V. Cell Wall Maturation of Arabidopsis Trichomes Is Dependent on Exocyst Subunit EXO70H4 and Involves Callose Deposition. *Plant Physiol.* **2015**, *168*, 120–131. [CrossRef] [PubMed]
42. Potikha, T.; Delmer, D.P. A Mutant of Arabidopsis Thaliana Displaying Altered Patterns of Cellulose Deposition. *Plant J.* **1995**, *7*, 453–460. [CrossRef]
43. Li, S.; Blanchoin, L.; Yang, Z.; Lord, E.M. The Putative Arabidopsis Arp2/3 Complex Controls Leaf Cell Morphogenesis. *Plant Physiol.* **2003**, *132*, 2034–2044. [CrossRef]
44. McKelvie, A.D. A list of mutant genes in arabldopsis thaliana (l.) heynh. *Radiat. Bot.* **1961**, *1*, 233–241. [CrossRef]
45. Marks, M.D.; Feldmann, K.A. Trichome Development in Arabidopsis Thaliana. 1. T-DNA Tagging GLABROUS1 Gene. *Plant Cell* **1989**, *1*, 1043–1050. [CrossRef]

46. Monnier, A. *Essai Monographique Sur Les Hieracium Et Quelques Genres Voisins*; Hissette: Nancy, France, 1829.
47. Zahradníček, J.; Chrtek, J. Cytotype Distribution and Phylogeography of *Hieracium Intybaceum* (Asteraceae): Cyto and Phylogeography of *Hieracium Intybaceum*. *Bot. J. Linn. Soc.* **2015**, *179*, 487–498. [CrossRef]
48. Grass, S.; Zidorn, C.; Ellmerer, E.P.; Stuppner, H. Eudesmane Derivatives from Hieracium Intybaceum. *Chem. Biodivers.* **2004**, *1*, 353–360. [CrossRef]
49. Haveman, R. Enkele opmerkelijke vondsten van Hieracium sabaudum L. s. str. op de Veluwe. *Gorteria* **2010**, *34*, 137–143.
50. Chrtek, J. Hieracium Decipientiforme (the H. Nigrescens Group)—An Interesting Species of the Ukrainian Carpathians. *Folia Geobot.* **1997**, *69*, 121–128.
51. Szeląg, Z. Taxonomic and Nomenclatural Notes on Hieracium Tubulare (Asteraceae) with Description of a New Species from the Eastern Carpathians. *Ann. Bot. Fennici.* **2006**, *43*, 310–314.
52. Albrechtová, J.; Kubínová, Z.; Soukup, A.; Janáček, J. Image Analysis: Basic Procedures for Description of Plant Structures. In *Plant Cell Morphogenesis: Methods and Protocols*; Cvrčková, F., Žárský, V., Eds.; Springer: New York, NY, USA, 2019; pp. 109–119, ISBN 978-1-4939-9469-4.
53. Gundersen, H.J.G.; Jensen, E.B. The Efficiency of Systematic Sampling in Stereology and Its Prediction. *J. Microsc.* **1987**, *147*, 229–263. [CrossRef]
54. O'Brien, T.P.; Feder, N.; McCully, M.E. Polychromatic Staining of Plant Cell Walls by Toluidine Blue O. *Protoplasma* **1964**, *59*, 368–373. [CrossRef]
55. Potůčková, M.; Červená, L.; Kupková, L.; Lhotáková, Z.; Lukeš, P.; Hanuš, J.; Novotný, J.; Albrechtová, J. Comparison of Reflectance Measurements Acquired with a Contact Probe and an Integration Sphere: Implications for the Spectral Properties of Vegetation at a Leaf Level. *Sensors* **2016**, *16*, 1801. [CrossRef]
56. Porra, R.; Thompson, W.; Kriedemann, P. Determination of Accurate Extinction Coefficients and Simultaneous-Equations for Assaying Chlorophyll-a and Chlorophyll-B Extracted with 4 Different Solvents—Verification of the Concentration. *Biochim. Biophys. Acta* **1989**, *975*, 384–394. [CrossRef]
57. Wellburn, A.R. The Spectral Determination of Chlorophylls a and b, as Well as Total Carotenoids, Using Various Solvents with Spectrophotometers of Different Resolution. *J. Plant Physiol.* **1994**, *144*, 307–313. [CrossRef]
58. Esbensen, K.; Swarbrick, B.; Westad, F.; Whitcomb, P.J.; Anderson, M.J. *Multivariate Data Analysis: An Introduction to Multivariate Analysis, Process Analytical Technology and Quality by Design*; CAMO Software AS: Oslo, Norway, 2018; ISBN 978-82-691104-0-1.
59. Zhao, N.; Wu, Z.; Zhang, Q.; Shi, X.; Ma, Q.; Qiao, Y. Optimization of Parameter Selection for Partial Least Squares Model Development. *Sci. Rep.* **2015**, *5*, 11647. [CrossRef]
60. Kopačková, V.; Ben-Dor, E.; Carmon, N.; Notesco, G. Modelling Diverse Soil Attributes with Visible to Longwave Infrared Spectroscopy Using PLSR Employed by an Automatic Modelling Engine. *Remote Sens.* **2017**, *9*, 134. [CrossRef]
61. Heise, H.M.; Damm, U.; Lampen, P.; Davies, A.N.; McIntyre, P.S. Spectral Variable Selection for Partial Least Squares Calibration Applied to Authentication and Quantification of Extra Virgin Olive Oils Using Fourier Transform Raman Spectroscopy. *Appl. Spectrosc. AS* **2005**, *59*, 1286–1294. [CrossRef]
62. Telfer, A.; Bollman, K.M.; Poethig, R.S. Phase Change and the Regulation of Trichome Distribution in Arabidopsis Thaliana. *Development* **1997**, *124*, 645–654. [CrossRef]
63. Hauser, M.-T.; Harr, B.; Schlötterer, C. Trichome Distribution in Arabidopsis Thaliana and Its Close Relative Arabidopsis Lyrata: Molecular Analysis of the Candidate Gene GLABROUS1. *Mol. Biol. Evol.* **2001**, *18*, 1754–1763. [CrossRef]
64. Schreuder, M.D.J.; Brewer, C.A.; Heine, C. Modelled Influences of Non-Exchanging Trichomes on Leaf Boundary Layers and Gas Exchange. *J. Theor. Biol.* **2001**, *210*, 23–32. [CrossRef]
65. Gottschlich, G.; Drenckhahn, D. Iconography of the Genus Hieracium in Central Europe—Part 1 General Description and Morphotypes. *Forum Geobot.* **2005**, *2*, 1–7.
66. Chrtek, J.; Mráz, P.; Belyayev, A.; Paštová, L.; Mrázová, V.; Caklová, P.; Josefiová, J.; Zagorski, D.; Hartmann, M.; Jandová, M.; et al. Evolutionary History and Genetic Diversity of Apomictic Allopolyploids in *Hieracium* s.Str.: Morphological versus Genomic Features. *Am. J. Bot.* **2020**, *107*, 66–90. [CrossRef]
67. Krak, K.; Mráz, P. Trichomes in the Tribe Lactuceae (Asteraceae)—Taxonomic Implications. *Biologia* **2008**, *63*, 616–630. [CrossRef]
68. Billings, W.D.; Morris, R.J. Reflection of Visible and Infrared Radiation from Leaves of Different Ecological Groups. *Am. J. Bot.* **1951**, *38*, 327–331. [CrossRef]
69. Shull, C.A. A Spectrophotometric Study of Reflection of Light from Leaf Surfaces. *Bot. Gaz.* **1929**, *87*, 583–607. [CrossRef]
70. Mershon, J.P.; Becker, M.; Bickford, C.P. Linkage between Trichome Morphology and Leaf Optical Properties in New Zealand Alpine Pachycladon (Brassicaceae). *N. Z. J. Bot.* **2015**, *53*, 175–182. [CrossRef]
71. Bell, C.C.; Curran, P.J. The Effect of Specular Reflectance on the Relationship between Reflectance and Vegetation Amount. *Int. J. Remote Sens.* **1992**, *13*, 2751–2757. [CrossRef]